

U.S. DEPARTMENT OF COMMERCE
National Technical Information Service

AD-A025 330

TECHNOLOGY AND PHYSICS OF INFRARED AND POINT
CONTACT DIODES

MASSACHUSETTS INSTITUTE OF TECHNOLOGY

PREPARED FOR
ROME AIR DEVELOPMENT CENTER

MARCH 1976

REPRODUCED BY
**NATIONAL TECHNICAL
INFORMATION SERVICE**
U. S. DEPARTMENT OF COMMERCE
SPRINGFIELD VA. 22161

Unclassified

SECURITY CLASSIFICATION OF THIS PAGE (When Data Entered)

REPORT DOCUMENTATION PAGE		READ INSTRUCTIONS BEFORE COMPLETING FORM
1. REPORT NUMBER RADC-TR-76-94	2. GOVT ACCESSION NO.	3. RECIPIENT'S CATALOG NUMBER
4. TITLE (and Subtitle) TECHNOLOGY AND PHYSICS OF INFRARED AND POINT CONTACT DIODES		5. TYPE OF REPORT & PERIOD COVERED Scientific Interim 1 May 75 - 31 Oct 75
		6. PERFORMING ORG. REPORT NUMBER Semi Annual Tech Rpt No. 3
7. AUTHOR(s) Ali Javan		8. CONTRACT OR GRANT NUMBER(s) F19628-74-C-0182
9. PERFORMING ORGANIZATION NAME AND ADDRESS Department of Physics Mass. Inst. of Tech. Cambridge, MA 02139		10. PROGRAM ELEMENT, PROJECT, TASK AREA & WORK UNIT NUMBERS 61101E 2001 01 01
11. CONTROLLING OFFICE NAME AND ADDRESS Defense Advanced Research Projects Agency 1400 Wilson Blvd Arlington, VA 22209		12. REPORT DATE March 1976
		13. NUMBER OF PAGES 44
14. MONITORING AGENCY NAME & ADDRESS (if different from Controlling Office) Deputy for Electronic Technology (RADC) Hanscom AFB, MA 01731 Monitor: Audun Hordvik/ETSL		15. SECURITY CLASS. (of this report) Unclassified
		15a. DECLASSIFICATION/DOWNGRADING SCHEDULE
16. DISTRIBUTION STATEMENT (of this Report) Approved for public release; distribution unlimited.		
17. DISTRIBUTION STATEMENT (of the abstract entered in Block 20, if different from Report)		
18. SUPPLEMENTARY NOTES This research was sponsored by the Defense Advanced Research Projects Agency, ARPA Order No. 2618		
19. KEY WORDS (Continue on reverse side if necessary and identify by block number) Tunneling resonances Dielectric formation Oxide studies Photoemission		
20. ABSTRACT (Continue on reverse side if necessary and identify by block number) Background work for this contract, performed by this laboratory, has shown that tunneling characteristics of junctions formed by a very thin dielectric layer sandwiched between two metals is independent of frequency (from DC through 10 μ wave length). Principal work done this period was on the optical response of Al-Al ₂ O ₃ -Al junctions. These demonstrated characteristic photoemission response with considerable bolometric effect. An analysis of the data showed that the model is consistent with experimental		

Unclassified

SECURITY CLASSIFICATION OF THIS PAGE(When Data Entered)

results and correctly predicts behavior at lower frequencies. Work was done on Al-Al₂O₃-Pb junctions in the far infrared at liquid nitrogen and liquid helium temperatures; equipment difficulties precluded obtaining new information. Three talks were given and three articles submitted for publication during this period.

Unclassified

SECURITY CLASSIFICATION OF THIS PAGE(When Data Entered)

TABLE OF CONTENTS

	<u>Page</u>
1. Summary	1
2. Introduction	2
3. Optical Response of Al-Al ₂ O ₃ -Al Junctions	3
4. Far Infrared Response of Lead on Aluminum Junctions	5
5. Near Infrared Mixing	5
6. Talks and Publications	5
7. Appendix A	A-1
8. Appendix B	B-1
9. Appendix C	C-1

1. SUMMARY

Background work for this contract, performed by this laboratory, has shown that tunneling characteristics of junctions formed by a very thin dielectric layer sandwiched between two metals is independent of frequency (from DC through 10 μ wave length). Principal work done this period was on the optical response of Al-Al₂O₃-Al junctions. These demonstrated characteristic photoemission response with considerable bolometric effect. An analysis of the data showed that the model is consistent with experimental results and correctly predicts behavior at lower frequencies. Work was done on Al-Al₂O₃-Pb junctions in the far infrared at liquid nitrogen and liquid helium temperatures; equipment difficulties precluded obtaining new information. Three talks were given and three articles submitted for publication during this period.

2. INTRODUCTION

Preliminary work in this laboratory has shown that tunneling characteristics of metal-oxide-metal junctions are essentially independent of frequency as long as photon energy is less than the barrier height. Recent calculations show the effects of circuit parameters on response of antenna/diode combinations; the junction capacitance is responsible for roll off in the infrared. Photo emission and bolometric effects are the dominant response in the visible region. Experimental evidence seems to be in accord with these calculations but true confirmation awaits additional measurements.

Important elements in device merit are junction non-linearity and even negative resistance which may be enhanced by choice of materials, techniques of application and operating temperature.

3. OPTICAL RESPONSE OF Al-Al₂O₃-Al JUNCTIONS

Initially, data were taken on low impedance junctions ($R_D \approx 100 - 500 \mu\Omega$). Thermal, bolometric, response contributed up to 300% of the faster photoelectric effect response. To eliminate the thermal response, short time radiation pulses were used. The optical spectrum investigated included six argon laser lines (5145A to 4579A). Pulse durations were 60 μ s, provided by a mechanical chopper wheel. Thermal responses increase exponentially in time; for small times this increase is roughly linear. Using a boxcar integrator with a small gate width of 5 μ s, two responses were taken; the zero time signal was obtained by linear extrapolation. The zero time signal, of course, will be due entirely to photoelectric response, since the thermal response is zero then.

This method of data collection was used to obtain Fowler plots at zero bias and for positive and negative bias levels up to 300 mV.

Fowler plots at zero bias yielded barrier heights from 1.7 eV to 2.4 eV on the junctions tested, depending on the junction tested.

In one case, this barrier height was compared to that obtained from the junction resistance and the familiar Stratton formulation of tunneling current:

$$R_D \approx \frac{1}{162} \frac{Se^8}{2A}$$

where $S = L\sqrt{\phi}$

L = barrier thickness in \AA

ϕ = mean barrier height in eV

A = junction area in $(\mu)^2$

The comparison was very good, which indicates that barrier characteristics remained essentially constant from D.C. to optical frequencies, although in the former case conduction is due to tunneling, while in the latter, it is due to photoelectric effect and classical barrier penetration.

These results are included in a paper "Mechanism of Detection of Radiation in a High-Speed Metal-Metal Oxide-Metal Junction in the Visible and Radiofrequency Regions" by Elchinger, et al., which is scheduled to be published in the January 1976 Journal of Applied Physics.

The thermal response can be reduced by increasing the junction resistance, at the expense of increased junction time constant. Again, from Stratton,

$$R_D(T) = R_0 \frac{\sin \beta T}{\beta T}$$

where $\beta = \frac{\pi L k_0}{\hbar(2m/\phi_0)^{1/2}}$
 T = temperature

$$\frac{\Delta R_D}{R_D} = -\frac{1}{3}(\beta T)^2 \frac{\Delta T}{T}$$

and for $T \approx 300^\circ K$,

$$\frac{\Delta R_D}{R_D} \approx -1.45 \times 10^{-4} \Delta T,$$

and for large R_D , ΔR will be small. Then the bolometric effect will be small for large R_D .

With the modification that junction resistance be large, either by increasing oxide thickness or decreasing junction area, it was found that photoresponse could be observed directly (without extrapolation) for zero bias and small voltages around zero bias ($\sim \pm 200$ mV).

4. FAR INFRARED RESPONSE OF LEAD ON ALUMINUM JUNCTIONS

Unsuccessful attempts to observe response of evaporated Al-Al₂O₃-Pb at 337 μ and liquid helium were made. In the early attempts, electrical noise from the laser made the observations difficult.

Electrical shielding was then added to the HCN laser and to the critical sensor elements preparatory to looking again for response of the junction to 337 μ radiation at liquid helium temperature. Electrical noise was sufficiently reduced that observations of signal below 1 μ V could be made, but the signal was not observed. Modifications were made to the laser that further improved its noise characteristics and smaller junctions were fabricated but dewar failure precluded additional runs this quarter. Dewar repair and additional runs are planned in the near future.

5. NEAR INFRARED MIXING

A He-Ne laser at 1.15 μ was assembled and operated. This is in preparation for some mixing experiments in the near infrared which only await some free dye laser time.

6. TALKS AND PUBLICATIONS

Talks by members of the group were given in Atlantic City, New Jersey (Frequency Control Symposium), La Jolla, California (Optical Electronics) and in Zurich, Switzerland (Conference on Infrared Physics). Two of these and a study of the response of metal-metal oxide-metal junctions are being published.

"High Speed Rectifying Junctions in the Infrared; Recent MIT Developments" appeared in the Proceedings of the 29th Annual Frequency Control Symposium, Atlantic City, New Jersey. It described progress in the development of metal-oxide-metal infrared diodes. Investigations have been made of the dielectric tunneling barrier formed between evaporated metallic layers and the enhancement of non-linearities by tunneling resonances. These non-linearities are a valuable spectroscopic tool and a potential means of increasing rectification efficiency. The mechanism of detection of visible radiation by a thin film MOM structure was studied. The text of this article appears as Appendix A.

"Optical Electronics: An Extension of Microwave Electronics into the Far Infrared and Infrared" is scheduled for publication in the Journal of Infrared Physics. It reviews the past activities at MIT in the area of extending frequency mixing and absolute frequency measurements in the infrared utilizing a high speed metal-metal oxide-metal junction. Recent developments in junctions deposited on a substrate are described. Emphasis is placed on the future possibilities of large arrays and potential use as high frequency oscillators and other active elements. The text of this article appears as Appendix B.

"Mechanism of Detection of Radiation in a High-Speed Metal Oxide-Metal Junction in the Visible" is scheduled for publication in the Journal of Applied Physics, January 1976. It describes a study of the mechanism of detection of radiation by a small-area thin film metal-metal oxide-metal structure.

After subtracting thermal effects, the response at optical frequencies is shown to arise from photoemission over the oxide's potential barrier. At lower frequencies the mechanism arises from a rectification process dictated by the nonlinear I-V characteristics due to electron tunneling across the junction. The text of this article appears as Appendix C.

A draft of an article has been written which relates fabrication parameters to microwave/infrared behavior of MOM diodes with integral antennas. This article presents computer calculations of circuit roll-off through the infrared. The detectivity at room temperature of a single structure can be as high as 10^{10} watts $^{-1}\text{Hz}^{1/2}$ at frequencies of 10^{14} . As a result, design guidelines are obtained for the lithographic fabrication of thin film MOM structures that can operate to the 10 micron region of the infrared spectrum. This article will be submitted for publication soon.

APPENDIX AHIGH SPEED RECTIFYING JUNCTIONS IN THE INFRARED: RECENT
M.I.T. DEVELOPMENTS*Introduction

The extension of microwave frequency synthesis techniques to the near infrared has been made possible by the development of a metal-oxide-metal point contact diode.^{1,2} Technologies have previously been described^{3,4} for printing, by using evaporation and photo-lithographic processes, integral antennas with rectifier/mixer diodes; these have been applied successfully in the far infrared. Attempts to operate them at still higher frequencies require smaller RC products or greater junction non-linearities. In mixing, difference frequencies may be severely limited by the RC products. Relatively large area (tens of square microns) are currently being used to investigate the barrier form and corrections due to finite conductivity of deposited metal, large dielectric constant of the substrate, and other effects. Usable junction non-linearities, in addition to those due to the tunneling process itself, arise from paramagnetic ions and specific impurities incorporated in the dielectric.

It is also possible to obtain rectification by photoelectric emission principally from one side of a junction. In this case, coupling into the junction is no longer by antenna and wavelengths coupled to the junction are not limited by junction RC.

Dielectric Formation

Much consideration has been given to methods of insulator

* This work has been supported by Air Force-ARPA Contract No. F 19628-74-C-0182.

formation since the problems are unique when thicknesses of the order of 10 Å are required. These dielectrics of roughly 10 atom layers thickness can permit essentially no pinholes, hence self grown oxides (or possibly nitrides or sulfides) appear the most promising approach. Oxide growth on a metal is dependent on the temperature of the metal, the partial pressure of oxygen above it, possible presence of water vapor, and the permeability of the oxide to oxygen diffusion. Plasma treatment may be given to the surface to either increase or reduce oxide thickness. Insulators that are evaporated, sputtered or deposited in some other way tend to form small islands and grow to cover the surface. Such layers inherently have pinholes until their thickness is several hundred Å.

Nickel oxide was used exclusively in our early investigations because the oxide is stable at about 10 Å. In order to study some tunneling resonances, our more recent work has been done principally with non-equilibrium oxidation of freshly evaporated aluminum with controlled oxygen pressures. Non-porous layers around 10 Å thickness have been formed. Diodes made by subsequent evaporation of a second metal have been sufficiently stable in room air to make consistent measurements. The barrier energy height may vary through even a very thin oxide layer and will also depend on oxygen availability at the growing interface, thus the Al-Al₂O₃-Al barrier may be asymmetric.

Tunneling Resonances

In addition to the normal electron tunneling other processes may take place. A tunneling electron may be inelastically scattered by an impurity in the dielectric;⁵ the electron

loses a certain amount of energy and the impurity molecule is left in an excited state with energy $h\nu$. This process can only occur if the junction is biased with a voltage $V > h\nu/e$. As a result of this, a structure appears in the plot of $\delta^2 J/\delta V^2$ versus the bias voltage, which except for the background, is similar to the infrared spectrum of the impurity molecules in the gas phase. (See Fig. 1). Because of the thermal smearing of the Fermi level of the electrodes, the use of cryogenic temperatures is necessary in order to improve the resolution of the resulting tunneling spectrum. In this way, we have observed tunneling resonances in aluminum-aluminum oxide-aluminum junctions.

This effect can be utilized in different ways. As a spectroscopic tool for chemical analysis it can give information on the impurity content of the dielectric in the tunneling junction. On the other hand, the enhanced non-linearities that result when the junctions are cooled to cryogenic temperatures will improve the performance on the MOM junctions as mixer elements.

Photoemission

The mechanism of detection of visible radiation by a thin film MOM structure⁶ has been studied.⁷ The response of an Al-Al₂O₃-Al junction was measured at various applied biases (to 0.3v) under irradiation successsively by six of the visible Ar laser lines. After subtracting thermal effects, the response at these optical frequencies was shown to arise from photoemission over the oxide's potential barrier, as previously demonstrated⁸ in work on slow speed large area junctions. At quantum energies less than the barrier height, the detection process is dominated by rectification due to the non-linear I-V

characteristics of electron tunneling across the junction.

Conclusion

The MOM point contact diode has made possible the extension of microwave techniques into the near infrared. Printed versions of these diodes promise to have a number of advantages over the mechanical point contact diodes, including stability, reproducibility, ability to integrate antenna arrays. Much work remains to be done in understanding the details of the electron tunneling process and in searching for MOM combinations with enhanced nonlinearities. The adoption of higher resolution microelectronic techniques can be expected to yield improved device performance at the shorter wavelengths. These advances have opened the way to the exciting new field of optical electronics.

References

1. Early work in this area is reviewed by A. Javan, in Fundamental and Applied Laser Physics, Proceedings of the Esfahan Symposium, August 1971, ed. by M.S. Feld, A. Javan, and N.A. Kurnit, Wiley-Interscience, New York (1973), p. 295.
2. A. Javan and A. Sanchez in Laser Spectroscopy, Proceedings of the Vail Conference, June, 1973, ed. by R. G. Brewer and A. Mooradian, Plenum, New York, 1974, p. 11.
3. J. G. Small, G. M. Elchinger, A. Javan, A. Sanchez, F. J. Banchner, and D. L. Smythe, Appl. Phys. Letts. 24, 275 (1974).
4. A. Javan and J. G. Small, in Proceedings of the 28th Frequency Control Symposium, Atlantic City, May 1974.
5. R. C. Jacklevic and J. Lambe, Phys. Rev. Letts. 17, 1139 (1966); Lambe and Jacklevic, Phys. Rev. Letts. 18, 821 (1968).

6. T. K. Gustafson, R.V. Schmidt and J. R. Perruca, Appl. Phys. Letts. 24, 620 (1974).

7. G. M. Elchinger, A. Sanchez, C. F. Davis, Jr., and A. Javan, to be published.

8. A. J. Braunstein, M. Braunstein and G. S. Picus, Appl. Phys. Letts. 8, 95 (1966).

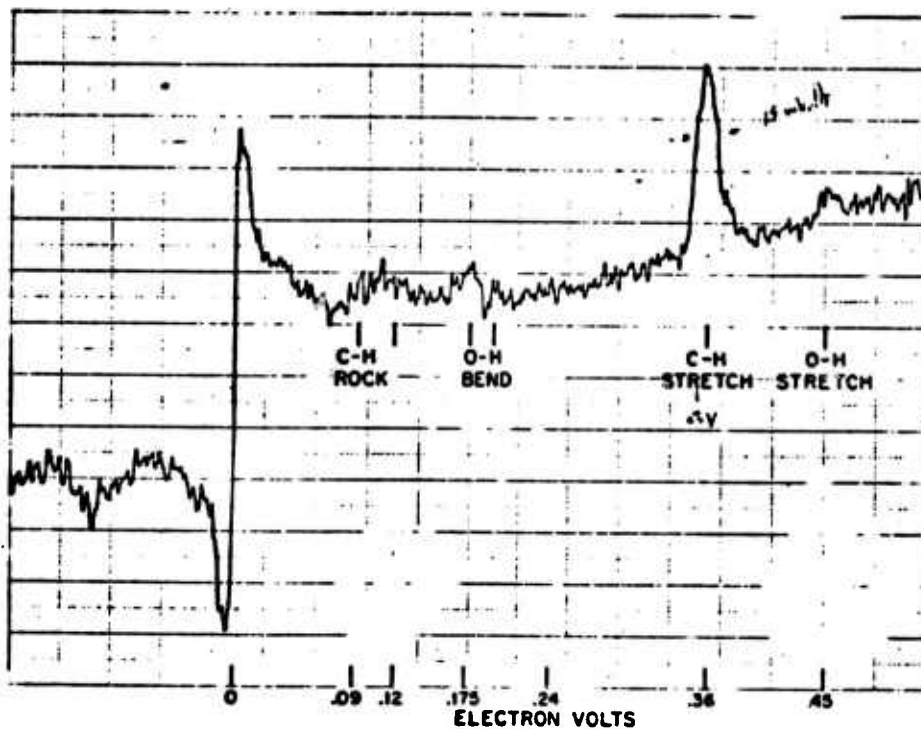


Fig. 1 Inelastic Tunneling in Al-Al₂O₃-Pb Junctions as Measured at 15 K.

APPENDIX BOPTICAL ELECTRONICS: AN EXTENSION OF MICROWAVE ELECTRONICS
INTO THE FAR INFRARED AND INFRAREDIntroduction

Radio and microwave electronics is the science of electronic devices operating on the principles of alternating currents flowing through the device elements. It includes the whole technology of classical electronics composed of vacuum tubes, solid state elements, lumped or distributed elements, oscillators, amplifiers, etc.

The concepts of quantum electronics are entirely different. Electrons resonating in atoms or molecules define the device operating characteristics. These quantum mechanical principles are the basis of currently existing maser oscillators and amplifiers, quantum counters, etc.

A circuit element will allow an alternating circuit to flow through it only if its time constant is less than or comparable with the period of the alternating frequency current. The time constant is determined by the element's inherent speed and the RC time constant of the lumped circuit to which it is coupled. In most microwave electronic circuits, the overall size of the element and its associated lumped circuit components must be less than the wavelength of signal(s) it is processing. This condition avoids problems due to phase shifts which can occur over distances larger than a wavelength when current through an element runs out of phase with respect to the voltage wave. In the microwave range it is often possible to distribute components over several wavelengths and design passive elements that periodically bring current in

phase with voltage.

In quantum electronics one does not usually think in these terms; however analogies exist -- for one, an atom or a molecule's time constant is sufficiently short, allowing it to respond to frequencies where its resonances lie. As for the phase consideration, we note that this is inherently a distributed system with atoms or molecules filling volumes with dimensions of several wavelengths. The atoms keep up with the spatial phase of the electromagnetic wave, according to the laws of stimulated emission of radiation or the phase matching criteria of the parametric processes. As a result, neither the time constant nor the phase requirements have presented any problem to extension of quantum-electronic devices into the optical regions; this became a reality with the advent of lasers early in the 1960's.

Extension of radio and microwave electronics into the optical region, however, required high speed elements of microscopic size, time constants less than an optical period and dimensions less than one light wavelength. Starting in the mid-1960's, in a continuing series of efforts,¹ we succeeded in making a two-terminal high-speed junction element capable of responding at extremely high frequencies. With it we have shown that it should be possible to extend the whole science of radio and microwave electronics into the far-infrared, infrared and eventually the visible regions. All of this work is still in its infancy, but it promises to open a whole new technology which we now identify as Optical Electronics. Other approaches which can be expected to contribute to this field include MOMOM triodes, superlattice and cryogenic Schottky negative resistance devices which can, in principle, operate at these frequencies and provide a whole class of active infrared devices.²

Point Contact Diodes

The metal-metal oxide-metal point contact diode consists of a sharply pointed wire whose tip is mechanically contacted to an oxidized flat surface. Rectification due to the non-linearities of quantum mechanical tunneling takes place at the junction which is the thin oxide layer below the sharp tip. Typically, a fifteen micrometer, tungsten wire is sharpened to a point less than 1000 Å in diameter and brought into contact with a polished nickel surface that has been oxidized under ambient conditions. Studies based on tunneling theory have shown that the oxide layer is typically about 10 Å thick. Coupling of the incident infrared radiation to the junction is through the whisker which acts as a multi-wavelength antenna with the expected large number of side lobes. The detailed antenna properties can be analyzed by considering the whisker and its image, in the nickel plane, as a long wire

antenna.

It should be noted that the conductance across the junction will normally present a somewhat higher resistance than the typical 100Ω antenna resistance. Capacitance for the assumed 10 \AA thick oxide with relatively small dielectric constant will be about 10^{-14} A (where $\text{A}(\mu\text{m})$ is for example 0.01). Thus the time constant of these junctions will be about 10^{-14} seconds. This is in the range of a period of visible light. Obviously the diode mount must be rigid and offer fine adjustment of the pressure at the whisker tip. Later we will see that these same expressions govern printed circuits with junctions formed by a small metal extension overlapping an original oxidized deposit.

Frequency Multiplication in the Infrared

The effect of non-linear junction characteristics may be seen to distort the current wave when a voltage sine wave is applied. This distortion expresses itself as harmonics. For many applications the second derivative will be the most important. In much of our work higher order mixing is desirable since we mix two laser signals and a microwave signal (often harmonics of these signals) to obtain a beat signal. In this fashion harmonics of stabilized klystrons have been used to measure the frequency of a far infrared HCN laser.³ This laser was in turn used to measure H_2O at $118\mu\text{m}$ ⁴ and D_2O at $84\mu\text{m}$.⁵ At the National Bureau of Standards the twelfth harmonic of the HCN laser was beat against a $28\mu\text{m}$ water vapor laser.⁶ This was used to measure CO_2 laser lines⁷ and finally a CO_2 harmonic was used to determine CO laser frequencies.⁸ Work at the National Bureau of Standards has extended this work to the HeNe $3.39\mu\text{m}$ line⁹ and the $2\mu\text{m}$ Xe line.¹⁰

Laser Phase Locking

A major part of our work was on developing techniques for producing a stable infrared frequency which could be phase-locked to the frequency standard. In order to compensate for laser frequency fluctuations, a microwave sideband was added to the laser frequency in the point contact diode and electrically tuned by means of a phase-locked frequency loop.¹¹ A harmonic of this stabilized frequency can then serve as the frequency reference in a subsequent step of the chain. In this way it is in principle possible to transfer all of the accuracy of the cesium standard to the near infrared region. In conjunction with laser frequency stabilization techniques like those described below, it is possible to conceive of new frequency standards of unsurpassed accuracy in the optical or infrared region.

The stabilization of CO₂ and N₂O lasers to the center of the Doppler profile of any of their transitions is made possible by monitoring the narrow saturation dip observed in 4.3-μm fluorescence from a low pressure absorber when a standing wave field is tuned to line center. We have been studying these resonances with a view toward achieving the narrow linewidth and high signal-to-noise ratio necessary for a stable frequency or wavelength source. With the use of an expanded beam to reduce power and transit-time broadening effects, and a large area He-cooled Cu:Ge detector, widths of less than 100 kHz (HWHM) have been obtained with signal-to-noise of ~200:1 at a pressure of only 1/2 mTorr.¹²

Sideband Reradiation at 10μm

An experiment has been performed at MIT which demonstrates conclusively that infrared currents do flow in antenna structures and diodes. In this experiment,¹³ the point contact diode is simultaneously irradiated with monochromatic infrared radiation from a CO₂ laser and microwaves from a V-band klystron. Currents across the junction are induced at the applied infrared and microwave frequencies and as a result of the non-linearities, currents will be generated at the sum and difference frequencies (first sidebands) and to a lesser extent at other frequency combinations. The presence of currents at the first side bands is demonstrated in the experiment by heterodyne detecting the radiation coming from the point contact at the corresponding first sideband frequencies. A detailed study showed that the amplitude of the currents generated at the first sidebands has the same bias dependence as the rectified 10 μm laser radiation. Furthermore, this dependence is shown to be the second derivative of the current with respect to the voltage as obtained from the static I-V characteristic. This, in fact, is expected if the same low frequency I-V characteristic dictates the performance at frequencies as high as the infrared.

Printed Diodes

"Printec diodes" have also been made.¹⁴ On a transparent substrate, the metallization areas are photolithographically defined and chrome overlayed with nickel is deposited. The nickel is oxidized in room air at room temperature and a second deposition is performed of nickel or gold on chrome where the chrome contacts underlying nickel oxide and acts as a glue to hold the metallization to the substrate. The nickel or gold enhances conduction. This forms the second half of the antenna structure and slightly overlaps the first deposition thereby forming the tunneling barrier diode. Comparing the antenna patterns at two HCN wavelengths shows that very considerable differences can exist over a small frequency range. These

devices have the advantage over point contact diodes of mechanical stability, reproducibility (in principle) and potentially the capability of being deposited in an array. It is possible to have arrays of several elements coupled into a single diode. One modification of the basic structure consisted of coupling a microwave and infrared dipole with the MOM diode so that the structure would be receptive to both frequencies. Mixing of a harmonic of 70 GHz with the 337 μm HCN line to yield a beat note was accomplished by this means.¹⁵

We feel that one unique feature of this work is realization that to function properly an infrared diode must have an extremely small cross sectional area and an extremely thin oxide. Tunneling resistance increases exponentially with dielectric thickness while capacitance goes as the reciprocal of thickness. Thus the RC product is minimized for the thinnest non porous oxide. But to retain a reasonably high resistance to avoid excessively loading the antenna, in these high speed junctions, the area must also be small. It is possible to find naturally grown oxides of the order of 10 Å thick. Nickel and tungsten form such layers at room temperature in ordinary air. Such layers can also be produced on other metals and they can be stable.

Photoemission

The response mechanism of MOM diodes has been shown to be quantum mechanical electron tunneling in the rf, microwave, submillimeter and in the infrared. But a different mechanism dominates in the visible. This is photoemission.

A study¹⁶ was made of an Al-Al₂O₃-Al junction fabricated by vacuum deposition through a mechanical mask. The response of this junction to the radiation of six of the visible argon laser lines was measured as a function of the applied bias voltage. Spurious signals arising from long time constant (>100 usec) thermal effects were subtracted (Fig. 1). The photoemissive signal appears across the junction as a voltage pulse with a rise and decay time following that of the incident laser pulse. This signal is observed only if the laser is focused at the edge of the junction where the oxide is exposed. The experimental results are all obtained with the power in each oscillating line set at 20 mw as measured on a calibrated power meter.

Photoemission occurs when the incident photon energy is greater than the barrier height. In the absence of bias it is known that the Al-Al₂O₃-Al barrier has an asymmetrical shape with the lower barrier height on the side of the first deposited metal.¹⁷ When the rate of electron excitation on either side of the barrier is the

same, the net photocurrent would be zero unless the propagating electrons suffer collisions in the dielectric. After a collision the presence of the intrinsic field would favor the flow of electrons from the high side, ϕ_2 , to the low side of the barrier. A net photocurrent would also result from differing rates of electron excitation on either side of the barrier. It can be shown that the photocurrent, I_{ph} , is given by $I_{ph} = A(hv - \phi_2)^2$ for $(hv - \phi_2) > kt$. Thus the voltage developed across the junction, V_s , is the product of photocurrent and tunneling impedance, R_d . Figure 2 displays the zero bias data of Fig. 1. Here $\sqrt{V_s}$ is plotted against frequency and data fit with a straight line is in excellent agreement with the photoemissive nature of the process. Intersection with the frequency axis of that straight line gives the maximum barrier height, $\phi_2 = 2.10 \pm 0.1\text{eV}$.

Inspection of the process shows that the photocurrent has a bias voltage dependence given by $I_{ph} = I_0 + m V_b$, where the slope, m , is proportional to $h\nu^2 \phi_2$. When the experimentally determined values for the slope, m , are plotted as a function of the frequency, they fall on a straight line whose intersection with the frequency axis should, again, give the value of the barrier height ϕ_2 . A value $\phi_2 = 2.12 \text{ eV}$ is obtained in this manner in close agreement with that reported above. Information obtained by studying the same junction at radio frequencies utilizing Stratton tunneling theory,¹⁸ can be used to yield more information on the barrier. The measured slope of current responsivity (the ratio between the rectified current and the radiofrequency power incident on the junction) at zero bias of 2.65 volt^{-2} and the measured junction impedance of $15 \text{ k}\Omega$ make it possible to calculate a barrier height of 2.1 eV and a barrier thickness of 13\AA . The value is in general agreement with experimental data¹⁷ ($\phi = 1.77 \text{ eV}$) obtained with a considerably thicker oxide formed by a different oxidation procedure.

Inelastic Scattering

Non-linearities of metal-oxide-metal diodes at room temperature can be satisfactorily understood on the basis of elastic tunneling of electrons across the potential barrier formed by the thin oxide layer. Although less likely the tunneling electron can be inelastically scattered by impurities existing in the oxide. As a result the tunneling electron gives up some of its energy and the impurity is excited to some vibrational level. If the impurity vibrational energy is $\hbar\omega_0$, the process will only have an appreciable probability if the bias voltage is $eV_b > \hbar\omega_0$. As a result it can be shown that there is step in the plot of the conductance versus bias voltage, corresponding to a change in conductance of about 1%. The second derivative $\partial^2 I / \partial V^2$ will consequently show a resonantlike structure at a voltage $eV = \hbar\omega_0$ with a width on the order of kT .

A small area, high speed junction in which inelastic tunneling takes place, would show interesting dispersive effects at frequencies in the infrared just above and below ω_0 . As a result the junction would present a voltage dependent reactance at certain infrared frequencies. Such a nonlinear reactance could be utilized in some types of parametric processes and devices could be built, for example, a parametric subharmonic oscillator. This requires integrating the device to some type of resonator at infrared frequencies. Rather than using a cavity or a Fabry-Perot, smaller than a wavelength structures could be built that present a high enough Q to allow oscillations.

References

1. "Extension of Microwave Detection and Frequency Measuring Technologies into the Optical Region," A. Javan and A. Sanchez, *Laser Spectroscopy*, edited by Brewer and Mooradian, Page 11, Plenum Press, 1975.
2. "Tunneling in a Finite Superlattice," *Appl. Phys. Letters* 22, 562 (1973); "Long Journey into Tunneling," L. Esaki, *Rev. of Mod. Physics* 46, 237 (1974); "Electron Tunneling and Superconductivity," J. Giaver, *Rev. of Mod. Physics* 46, 245 (1974).
3. "Absolute Frequency Measurement of New cw HCN Submillimeter Laser Lines," L.O. Hocker and A. Javan, *Phys. Letters* 25A, 489 (1967).
4. "Laser Harmonic Frequency Mixing of Two Different Far IR Laser Lines up to 118 μ ," L.O. Hocker and A. Javan, *Phys. Letters* 26A, 6 (1968).
5. "Extension of Absolute Frequency Measurement to the 84 μ Range," L.O. Hocker, J.G. Small, and A. Javan, *Phys. Letters* 29A, 321 (1969).
6. "Absolute Frequency Measurement of the 28 μm and 78 μm cw Water Vapor Lines," K.M. Evenson, *Appl. Phys. Letters* 16, 159 (1970).
7. "Extension of Laser Harmonic Frequency Mixing Techniques into the 9 μ Region with an Infrared Metal Point-Contact Diode," V. Daneu, D. Sokoloff, A. Sanchez and A. Javan, *Appl. Phys. Letters* 15, 398 (1969); "Absolute Frequency Measurement of the CO₂ cw Laser at 28 THz (10.61 μm)," K.M. Evenson, J.S. Wells and L.M. Matarrese, *Appl. Phys. Letters* 16, 251, (1970).
8. "Extension of Laser Harmonic Frequency Mixing into the 5 μ Region," D. Sokoloff, A. Sanchez, R. Osgood, A. Javan, *Appl. Phys. Letters* 17, 257 (1970).

9. "Accurate Frequencies of Molecular Transitions Used in Laser Stabilization: the 3.39 μm Transition in CH_4 and the 9.33 and 10.18 μm Transitions in CO_2 ," K.M. Evenson, J.S. Wells, F.R. Pettersen, B.L. Danielson and G.W. Day, *Appl. Phys. Lett.* 22, 192 (1973).
10. "Extension of Absolute Frequency Measurements to 148 THz: Frequencies of the 2.0 - and 3.5- μm Xe Laser," D.A. Jennings, F.R. Petersen and K.M. Evenson, *Appl. Phys. Letters*, 26, 510 (1975).
11. "Precision Absolute Frequency and Wavelength Measurements in the Infrared: A Review of Activities at MIT," J.G. Small, J.-P. Monchalin, M.J. Kelly, F. Keilmann, A. Sanchez, S.K. Singh, N.A. Kurnit, A. Javan, and F. Zernike, *Proceedings of the 26th Annual Frequency Control Symposium*, Atlantic City, June 1972.
12. "Standing Wave Saturation Resonances in the CO_2 10.6 μm Transitions Observed in a Low Pressure Room Temperature Absorber Gas," C. Freed and A. Javan, *Appl. Phys. Letters* 17, 53 (1970).
13. "Potential Frequency Accuracy of the CO_2 Fluorescence Saturation Dip," M.J. Kelly, J.E. Thomas, J.-P. Monchalin, N.A. Kurnit, and A. Javan, *Proceedings of the 29th Annual Frequency Control Symposium*, Atlantic City, May, 1975 (in press).
14. "Generation of Infrared Radiation in a Metal-to-Metal Point Contact Diode at Synthesized Frequencies of Incident Fields; A New High Speed Broad Band Light Modulator," A. Sanchez, S.K. Singh and A. Javan, *Appl. Phys. Letters* 21, 240 (1970).
15. "A.C. Electron Tunneling at Infrared Frequencies; A Thin Film M-O-M Diode Structure with Broad-Band Characteristics," J.G. Small, G.M. Elchinger, A. Javan, A. Sanchez, F.J. Bachner, and D.L. Smythe, *Appl. Phys. Letters* 24, 275 (1974).
16. "Mechanism of Detection of Radiation in a High-Speed Metal-Metal Oxide-Metal Junction in the Visible and Radiofrequency Regions," G.M. Elchinger, A. Sanchez, C.F. Davis, Jr., and A. Javan, to be published.
17. "Voltage Dependence of the Barrier Heights in Al_2O_3 Tunnel Junctions," A.J. Braunstein, M. Braunstein and G.S. Picus, *Appl. Phys. Letters* 8, 95 (1966).
18. "Volt-Current Characteristics for Tunneling Through Insulating Films," R. Stratton, *J. Phys. Chem. Solids* 23, 1177 (1962).

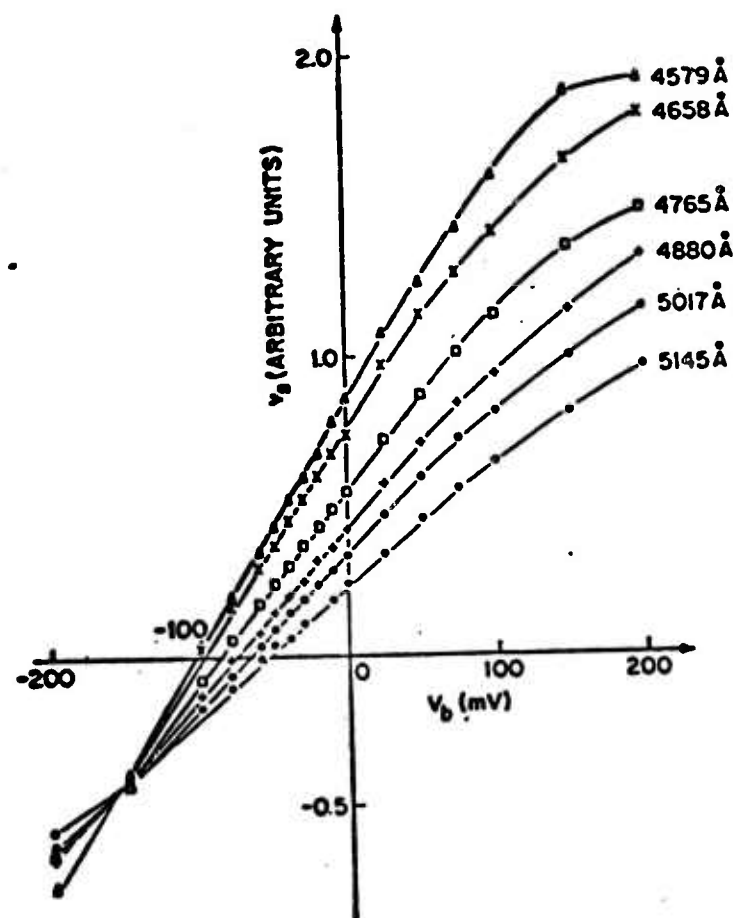


Figure 1. Photoresponse of small area Al-Al₂O₃-Al junction versus applied bias voltage at different wavelength radiations. For $(hv - \phi_2) > kT$, $(hv - \phi_2) \propto I_{ph}$, as shown in Fig. 2.

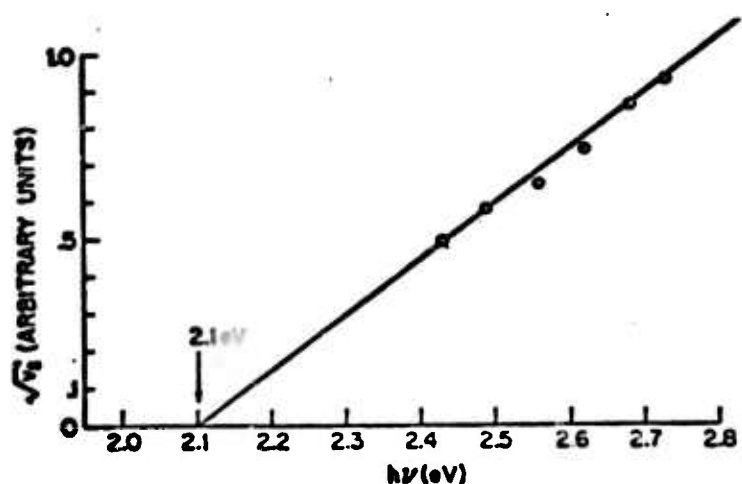


Figure 2. Fowler plot of zero bias data from Fig. 1. Square root of the response voltage is plotted against photon energy and best straight line is drawn through the data. The zero response value is the barrier height.

APPENDIX C

MECHANISM OF DETECTION OF RADIATION IN A HIGH-SPEED
METAL-METAL OXIDE-METAL JUNCTION IN THE VISIBLE AND RADIO-
FREQUENCY REGIONS*

* This work has been supported by AIR FORCE - ARPA Contract
No. F19628-74-C-0182.

The response to visible radiation of a small area thin film metal-oxide-metal (MOM) structure as well as that of a mechanical metal-to-metal point contact diode, has been previously reported.⁽¹⁻⁴⁾ For these, different possible mechanisms have been discussed, including optical rectification due to the nonlinear character of the electron tunneling process; this rectification process would be similar to that occurring at the infrared and the lower frequencies. This letter gives the results of an experiment in a high speed (small area) thin film deposited junction which shows that the response to optical frequencies arises from photoemission over the oxide's potential barrier and has the same origin as that observed sometime ago in a slow speed, large area junction.⁽⁵⁾ At lower frequencies, however, the mechanism is shown to arise from a rectification process dictated by the nonlinear I-V characteristic due to electron tunneling across the junction. This letter also gives new information on the photoemission process, not previously reported.

In the experiment, the response of the MOM junction at room temperature to the visible radiation obtained from an argon laser is studied as a function of a bias voltage applied to the junction and the frequency of the incident radiation. Nine different lines of the argon laser ranging from 4579\AA to 5145\AA are used. The measurement technique adopted in the experiment discriminates against spurious

signals appearing across the junction due to thermal effects which have a long time constant (exceeding about 100 μ sec). The results are then compared to the rectification of a radio frequency signal observed in the same junction versus a bias voltage. The barrier parameters obtained from photo-emission theory applied to the visible radiation response are found to be in excellent agreement with the parameters obtained from electron tunneling giving rise to the nonlinear I-V characteristic responsible for the rectification of the radiofrequency signal.

The studies are made in an Al-Al₂O₃-Al evaporated junction, fabricated by vacuum deposition through a mechanical mask. An Al strip 20 μ wide and 1000 \AA thick is first deposited and, after oxidation by exposure to ambient atmosphere for a few minutes, a similar Al strip is deposited forming with the first one a cross-like structure. The resulting impedance is in the k Ω range.⁽⁶⁾

In the experiment the output of the argon laser oscillating in a single line is focused onto the junction with a spot size of 5 microns. A mechanical chopper placed at the focus of two equal achromatic confocal lenses generates 60 μ sec pulses with a rise time of 2 μ sec and a duty cycle of about 20. The voltage appearing on the junction due to the laser pulse is averaged with a boxcar integrator at two times during the pulse and extrapolated back to the beginning of the pulse. In this way the signal across the junction due to the slow laser-induced thermal effects are subtracted. The

thermal signal originates from a bolometric process which is nearly proportional to the bias voltage across the junction. In fact, this signal becomes dominant and larger than the photoemissive signal for bias voltages exceeding about .1 volt.

The photoemissive signal appears across the junction as a voltage pulse with a rise and decay time following that of the incident laser pulse. This signal is observed only if the laser is focused at the edge of the junction where the oxide is exposed. The slow bolometric effect, however, is observed as long as the laser is focused on the junction or anywhere within a few microns of the junction. This effect is due to heating of the junction causing a decrease of the tunneling impedance.⁽⁷⁾ This observation is in general agreement with the types of signals reported in Ref. 1.

The experimental results reported below for six different laser lines are all obtained with the power in each oscillating laser line attenuated to the same power level, 20 mw, as measured with a calibrated power meter.

The experimental results are presented in Fig. 1a where the detected voltage, v_s , is plotted for a given frequency, as a function of the bias voltage. This family of curves also gives the response versus the frequency at various bias voltages, v_b , and contains information on the mechanism occurring in the junction.

The photoemission process occurs when the incident photon energy is higher than the barrier height. In this case the electrons in the metal on each side of the barrier are excited to an energy above the top of the barrier. The excited electrons can then propagate across the barrier in either direction. Consider first the photoemission process in the absence of an applied bias voltage. For an Al-Al₂O₃-Al junction, it is known that the barrier has an asymmetrical shape with the lower barrier height on the side of the first deposited metal (see barrier shape in Fig. 2).⁽⁵⁾ It is also known that for the case where the rate of electron excitation on either side of the barrier is the same, the net photocurrent would be zero unless the propagating electrons suffer collisions in the dielectric. After a collision the presence of the intrinsic field would favor the flow of electrons from the high side to the low side of the barrier. It is also to be noted that a net photocurrent would result if the rate of electron excitation differs on either side of the barrier. For both cases it can be shown that the photocurrent, I_{ph} , is given by $I_{ph} = A(h\nu - \phi_2)^2$. This formula holds when $h\nu - \phi_2 \gg kT$. Accordingly, the voltage developed across the junction, v_s , would be the product of the photocurrent times the tunneling impedance, R_d .

Figure 1b displays the data in Fig. 1a for zero bias ($v_b = 0$). In this figure, $\sqrt{v_s}$ is plotted versus frequency. The fit of the data with a straight line is in excellent

agreement with the photoemissive nature of the process.

The intersection with the frequency axis gives the maximum barrier height $\phi_2 = 2.10 \pm 0.1 \text{ eV}$

The above behavior is similar to that observed in large area junctions in which the second deposited metal was sufficiently thin to allow the applied radiation to penetrate through the thickness of the metal. In that experiment⁽⁵⁾ the measured maximum barrier height, ϕ_2 , for an Al-Al₂O₃-Al junction was 1.77eV. The difference we attribute to different oxidation procedure.

The slopes of the curves presented in Fig. 1a can also be used to obtain a precise measure of the barrier height; it can be shown that in the presence of a small bias voltage, the contribution to the net photocurrent from photoelectrons originated in side 1 (see Fig. 2) is changed while that from side 2 remains essentially unaffected. As a result, the photocurrent has a bias dependence that in the first approximation is linear and given by $I_{ph} = I_0 + mV_b$ where $m \propto (h\nu - \phi_2)$. Figure 1c displays the slope, m , versus $h\nu$ as obtained from the data points given in Fig. 1a. Notice that the intersection with the frequency axis gives again a measure of the barrier height $\phi_2 = 2.12 \pm 0.1 \text{ eV}$ in excellent agreement with the above results. This effect has not been reported previously and is highly useful for determining barrier height.

The curvature of the curves in Fig. 1a arises in part from the decrease in the tunneling impedance as a function of current. Furthermore, at higher voltages the lowering of the barrier height becomes an appreciable effect and contributes to the observed curvatures. Inspection of the data in Fig. 1a for large bias voltages is in general agreement with this effect.⁽⁸⁾

The response of a small area deposited metal-oxide-metal junction to infrared radiation has recently been observed and shown to be the same as the response obtained in the far infrared, microwaves or the radiofrequency regions.⁽⁹⁾ This arises from the rectification process predicted by the nonlinear I-V characteristic of the junction. For a junction of the dimensions used in this experiment, the capacitance is sufficiently low to allow appreciable coupling of the junction to a radiofrequency or microwave signal. The current responsivity, β_i , defined as the ratio between the rectified current, i_r , and the radiofrequency power, P , coupled to the junction ($\beta_i = i_r/P$) is determined by the local value of the second derivative of the junction's I-V characteristic at the point of operation ($\beta_i = \frac{1}{2} \left. \frac{\partial^2 I}{\partial V^2} \right|_{V_b} R_d$ where R_d = junction's resistance). Figure 3, therefore, displays the current responsivity versus the

applied bias voltage, V_b . For the above junction, the measured β_i for $V_b = 0$ is 0.087 volt^{-1} for a measured junction impedance of $R = 15k\Omega$.

In the same manner that has been shown for mechanical metal-to-metal point contact diodes⁽¹⁰⁾, it is possible to obtain the potential barrier parameters from the above measurements by direct application of the results of the electron tunneling theory. It can be shown⁽⁷⁾ and is in agreement with the experimental results that for small bias voltages the junction's responsivity has a linear dependence on the bias voltage given by $\beta_i = \beta_i(V_b=0) + u V_b$. From Fig. 3 we find that $u = 2.65 \text{ volt}^{-2}$. From the tunneling theory u and R_d are found to be functions of the average barrier height, ϕ_0 , and thickness, L given by $u = \frac{1}{2} (S/4\phi_0)^2$ and $R_d = S e^S / (324\phi_0 a)$. The junction's area, a , is given in (microns^2), R_d in ohms and S is a dimensionless parameter given by $S = 1.02L\sqrt{\phi_0}$ with L in angstroms and ϕ_0 in electron volts. Solution of the above equations using our measured values: $u = 2.65 \text{ volt}^{-2}$ and $R_d = 15k\Omega$ gives: $\phi_0 = 2.1 \text{ eV}$ and $L = 13\text{\AA}$. Note the agreement between this value of the barrier height and that obtained from measurement at optical frequencies.

The above agreement between the measured values of the barrier height is a striking demonstration that the same potential barrier that determines the properties of the junction at a radiofrequency also determines the behavior at optical frequencies. These properties arise from related, thought different, types of quantum mechanical processes.

In the case where the frequency of the applied radiation is comparable to the barrier height, the contribution to the photocurrent due to photon assisted tunneling can become quite important. It can be shown that, even in the present work, in which $h\nu - \phi_2$ was about 0.5eV the contribution due to photoelectrons with energies below the top of the barrier amounts to 5 to 10% of the total photocurrent. These and other related details will be published separately.

REFERENCES

1. T. K. Gustafson, R. V. Schmidt and J. R. Perruca, Appl. Phys. Letters 24, 620 (1974).
2. S. Faris, T. K. Gustafson and J. Wiesner, IEEE J. Quantum Electron. QE-9 737 (1973).
3. S. Y. Wang, S. M. Faris, D. P. Siu, R. K. Jain and T. K. Gustafson, Appl. Phys. Letters 25, 493 (1974).
4. Bor-long Twu and S. E. Schwarz, Appl. Phys. Letters 25, 595 (1974).
5. A. J. Braunstein, M. Braunstein and G. S. Picus, Appl. Phys. Letters 8, 95 (1966).
6. The resistance of the junction depends on the thickness of the oxide layer which in turn is dependent on the method of oxidation including the temperature and length of time of exposure to oxygen. Controlled oxidation process can be used to obtain lower impedance.
7. R. Stratton, J. Phys. Chem. Solids 23, 1177 (1962).
 The tunneling conductance per unit area is $G(T) = G_0 \frac{x}{\sin x}$
 where $G_0 = G(T=0)$ and $x = \frac{\pi}{2} \frac{L}{\sqrt{\phi}} kT$ for a trapezoidal barrier model. For $x \ll 1$ (otherwise thermionic emission would take place rather than tunneling) we have that the corresponding resistance depends on T as

$$R(T) = \frac{1}{G(T)} = R_0 \frac{\sin x}{x} \approx R_0 \left(1 - \frac{x^2}{6}\right)$$
 for $L = 13 \text{ \AA}$, $\phi = 2 \text{ eV}$
 and $T = 300^\circ\text{K}$ we have $x^2 = .13$ and $\frac{\Delta R}{R} = - \frac{x^2}{3} \frac{\Delta T}{T} = - 1.45 \times 10^{-4} \Delta T$
 so that if $\Delta T = 70^\circ\text{K}$, then $\frac{\Delta R}{R} \approx 10^{-2}$
8. A detailed analysis of this effect will be presented in a subsequent publication.
9. J. G. Small, G. M. Elchinger, A. Javan, A. Sanchez, F. J. Bachner, D. L. Smythe, Appl. Phys. Letters 24, 275 (1974).
10. A. Javan and A. Sanchez, Laser Spectroscopy, proceedings of the Vail Symposium p. 11, edited by R. G. Brewer and A. Mooradian, Plenum Press (1974).

FIGURE CAPTIONS

Figure 1. (a) Photoresponse of small area Al-Al₂O₃-Al junction versus applied bias voltage at different wavelength radiations. For $(h\nu - \phi_2) \gg kT$, $(h\nu - \phi_2) \propto \sqrt{I_{ph}}$, as shown in (b). These points are taken from (a) at $V_b = 0$. (c) shows the linear behavior of the slope of I_{ph} versus incident photon energy around zero bias. This indicates that for small applied bias voltage, the net change in the photocurrent is a linear function of V_b .

Figure 2. (a) Potential barrier shape at zero bias modeled from a basic trapezoid. Electrodes 1 and 2 are the first and second deposited Al strips, respectively. ϕ_2 is the larger barrier potential as determined experimentally. (b) Barrier altered by applied (positive) bias on electrode 1. At $T \approx 0^{\circ}\text{K}$, the maximum photoexcited electron energy will be $h\nu$ above each Fermi level.

Figure 3. Display of the current responsivity, β_i , versus applied bias voltage, V_b . By definition $\beta_i = i/P$ where P is the radiofrequency power coupled to the diode and is given by $P = \frac{V_{rf}^2}{R_d}$. Therefore $\beta_i = \frac{V_r}{V_{rf}^2}$ and is determined from the experiment by measuring the coupled radiofrequency voltage, V_{rf} , (r.m.s. value) and the resulting rectified voltage, V_r .

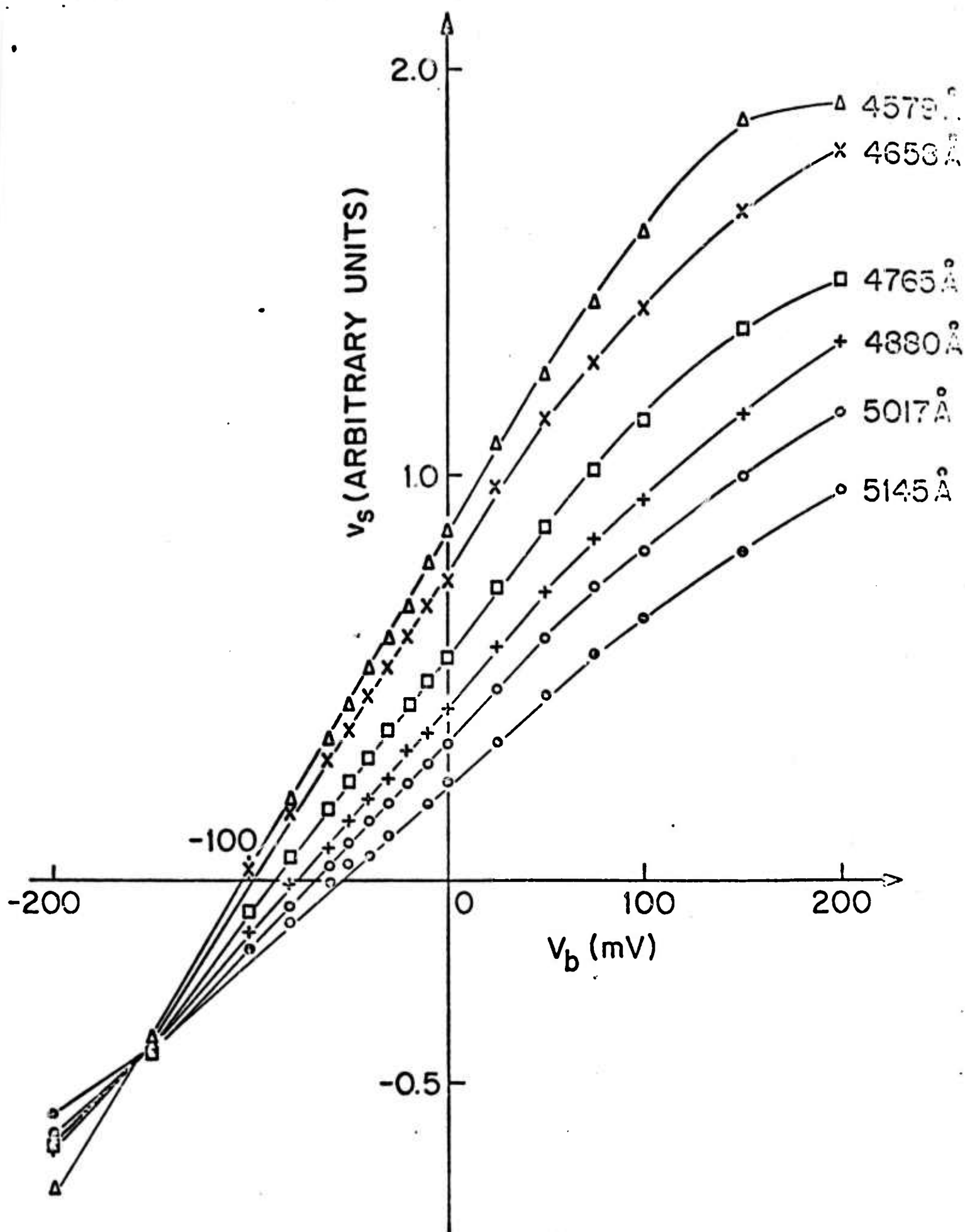
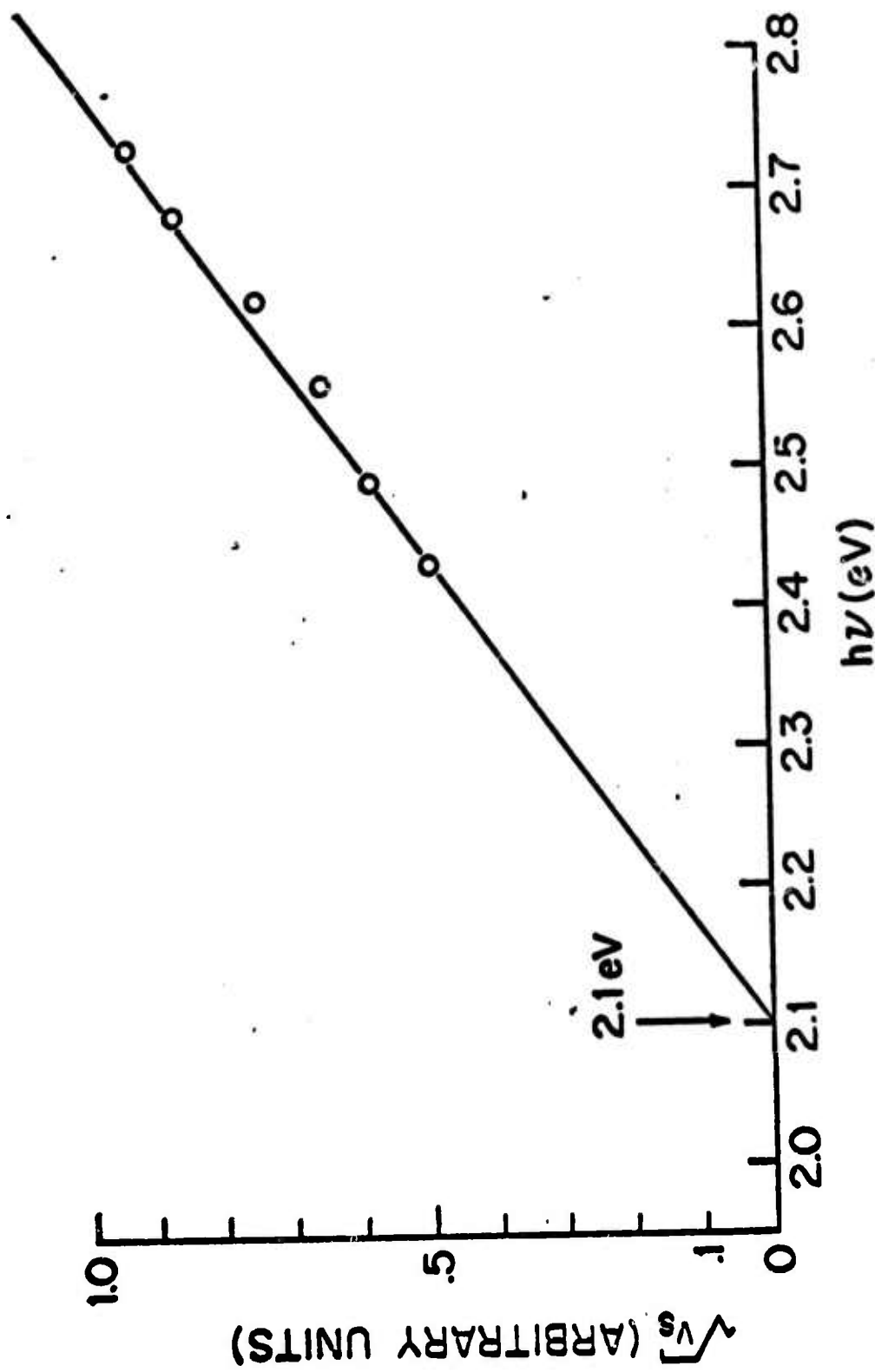


Fig. 1a

Fig. 1b



C²14

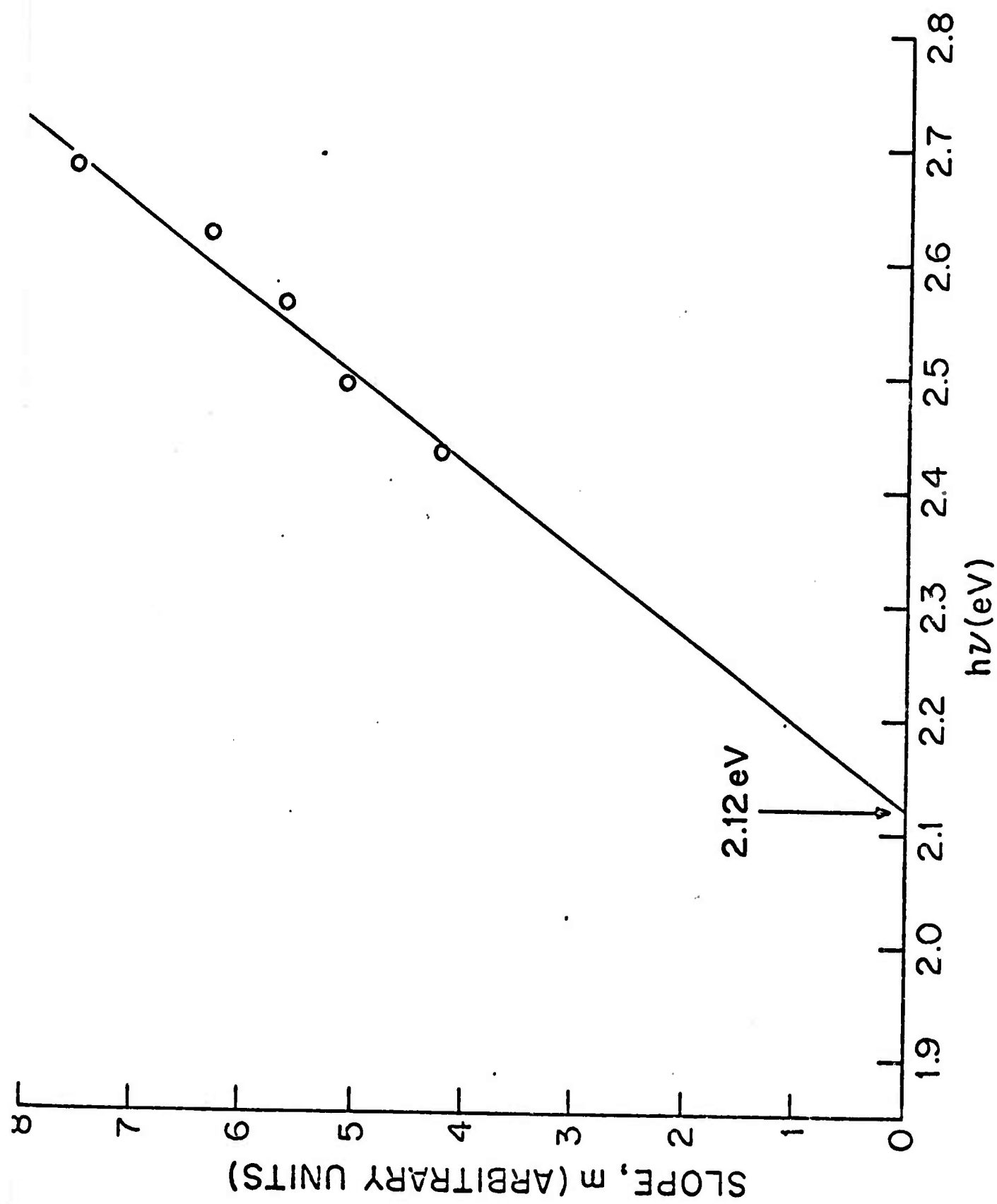


Fig. 1c

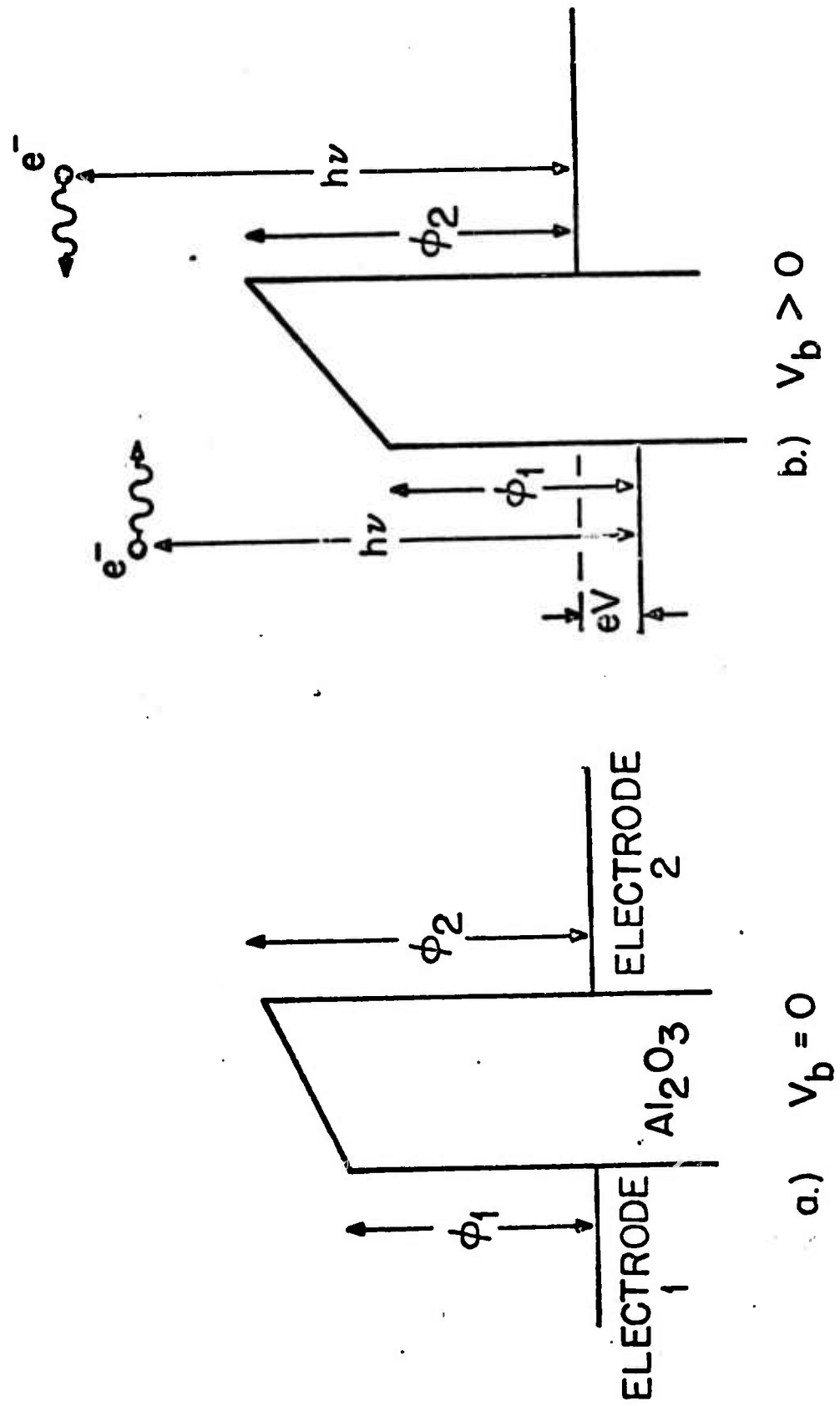


Fig. 2

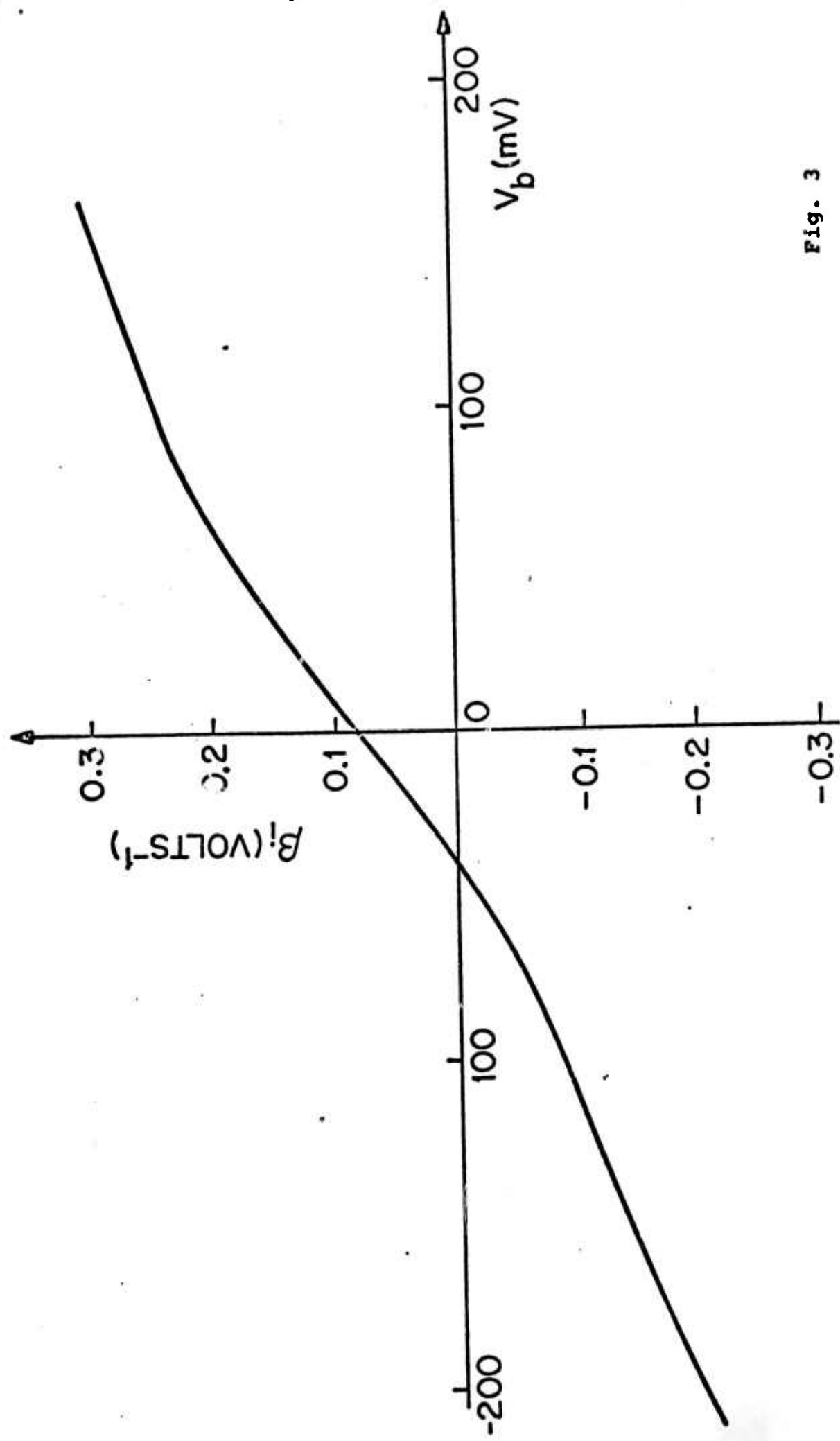


Fig. 3